Copyright Warning & Restrictions

The copyright law of the United States (Title 17, United States Code) governs the making of photocopies or other reproductions of copyrighted material.

Under certain conditions specified in the law, libraries and archives are authorized to furnish a photocopy or other reproduction. One of these specified conditions is that the photocopy or reproduction is not to be "used for any purpose other than private study, scholarship, or research." If a, user makes a request for, or later uses, a photocopy or reproduction for purposes in excess of "fair use" that user may be liable for copyright infringement,

This institution reserves the right to refuse to accept a copying order if, in its judgment, fulfillment of the order would involve violation of copyright law.

Please Note: The author retains the copyright while the New Jersey Institute of Technology reserves the right to distribute this thesis or dissertation

Printing note: If you do not wish to print this page, then select "Pages from: first page # to: last page #" on the print dialog screen

ABSTRACT

PHASE TUNABILITY IN A CONDUCTOR BACKED COPLANAR WAVEGUIDE PATCH ANTENNA

by
Idan Mandelbaum

Traditionally beam steering in phase array antenna systems is achieved using tunable phase shifters or switched feed networks. Here, a tunable patch antenna element is suggested as a novel alternative to a combination of a radiating element and a phase shifter. A conductor backed coplanar waveguide patch antenna is chosen due to its suitability to mounted external tuning elements, using varactor diodes. Limited types of lumped tuning circuits, using varactor diodes, have been tested, though a lumped as well as distributed tuning is feasible in the chosen antenna configuration. Approximate analytical models for coplanar waveguide patch antennas with finite ground plane have been developed; in the literature, such approach is limited to infinite ground plane coplanar waveguide patch antenna only. Numerical results from approximate model were used as initial values in optimized simulations using IE3D software tool. Coplanar waveguide patch antennas were constructed; re-tuned to the desired frequency and tuning element were surface mounted. Experimental measurements for input return loss and phase variation as a function of frequency are carried out using various bias voltages applied in tuning circuits. Despite observed small losses and incremental changes in the resonance frequency, significant phase shifts were obtained within the desired bandwidth (low VSWR.) Alternative tuning with ferroelectric elements and distributed tuning is suggested as further research.

PHASE TUNABILITY IN A CONDUCTOR BACKED COPLANAR WAVEGUIDE PATCH ANTENNA

by
Idan Mandelbaum

A Thesis
Submitted to the Faculty of
New Jersey Institute of Technology
in Partial Fulfillment of the Requirements for the Degree of
Master of Science in Electrical Engineering

Department of Electrical and Computer Engineering

August 2000

APPROVAL PAGE

PHASE TUNABILITY IN A CONDUCTOR BACKED COPLANAR WAVEGUIDE PATCH ANTENNA

Idan Mandelbaum

Dr. Ibrahim Akduman **Date**
Dean of Electrical and Electronics Engineering, Istanbul Technical University

---

Dr. Gregory Kriegsman **Date**
Professor of Mathematics, NJIT

Dr. Edip Niver, Thesis Adviser **Date**
Associate Professor of Electrical Engineering, NJIT

Dr. Bruce Nyman **Date**
Director of Advanced Technologies, JDS Uniphase, Inc.

BIOGRAPHICAL SKETCH

Author: Idan Mandelbaum

Degree: Master of Science in Electrical Engineering

Date: August 2000

Undergraduate and Graduate Education:

- Master of Science in Electrical Engineering,
  New Jersey Institute of Technology, Newark, NJ, 2000

- Bachelor of Science in Electrical Engineering,
  New Jersey Institute of Technology, Newark, NJ 1999

Major: Electrical Engineering

To my family.

ACKNOWLEDGMENT

The author wishes to express his gratitude to his advisor, Professor Edip Niver, for his guidance, friendship, and moral support throughout this research. Special thanks to Dr. Richard V. Snyder of R.S. Microwave and Dr. Anvar Zakhidor for the suggestions and constructive criticism as the research progressed. The author is greatful for Dr. Jian X. Zheng of Zealand Software, Inc for fast response to questions about IE3D and the donation of the software package. In addition the author would like to thank Dr. Ibrahim Akduman, Dr. Gregory Kriegsman, and Dr. Bruce Nyman for serving on the committee. Thanks also go out to Dr. Lale Alatan who helped a great deal in the early phase of the work and with the use of the IE3D software.

The author is grateful to the New Jersey TIDE Center at NJIT funded by New Jersey Commission on Science and Technology for providing the financial support.

TABLE OF CONTENTS

LIST OF FIGURES

CHAPTER 1

INTRODUCTION

In today's technological world, mobile telecommunication services plays a very critical part, anywhere from cellular phones, personal digital assistants to the Global Positioning System applications. Information must be accessible to millions of consumers anywhere in the world regardless of the environment. The effective radiation and reception of electromagnetic signals in all wireless applications depends on antenna effectiveness in terms of design characteristics.

Effective antennas are impedance matching devices; they match the impedance of the circuit to that of the medium and thereby providing an efficient means of radiating the signal into the medium or receiving the signal. The applications mentioned above, especially mobile applications require miniaturizations, imposing strict constraints on the size, gain and cost of the antenna while maintaining efficiency. To achieve the high efficiency and low cost of manufacturing, an attractive alternative is to implement the antenna on the printed circuit board that the handheld transceiver operates, or ideally on the chip itself that manages the communication, thus lowering manufacturing cost. A promising approach is to use a coplanar waveguide patch antenna, which effectively uses the surrounding ground plane to achieve better performance [1].

Analytical approximations are developed in this thesis, which give the dimensions to construct a conductor backed coplanar patch antenna. An attempt is made to design tunable antennas to replace the antenna element and phase shifter combination widely used in phase array antenna, such as reception antennas on cell towers or any other

multi-user tracking applications. Such approach will not only help to reduce the cost and part count but also will lead to greater miniaturization.

The Method of Moments is a numerical analysis tool based on integral equation solutions for a particular class of problems (Appendix A). In this thesis, the software tool IE3D, based on method of moment solution of multi-layered dielectric and conductors is used as a reference to compare developed analytical approximations for the coplanar waveguide patch antenna. Software simulations yield relatively accurate results. Extensive simulations are needed to obtain physical insight to the problem, where as analytical approximate results are much more efficient in this respect.

Conductor backed coplanar patch antennas were designed using analytical expressions developed here. Obtained analytical results were used as initial values for further optimization using IE3D software tool. Then antennas were fabricated on thin and thick substrates, tuning elements mounted and testing was carried out including measurements in an anechoic chamber for radiation patterns and insertion loss on the network analyzer (Appendix B).

CHAPTER 2

CONDUCTOR BACKED COPLANAR WAVEGUIDE PATCH ANTENNAS

Conductor backed coplanar waveguide antennas are relatively new addition to the planar circuit toolkit. The coplanar backed waveguide patch antennas share the same advantages of the conventional microstrip antennas, such as: low profile, light weight, easy manufacturing, lower cost and easily conform to tight spaces. They also offer many advantages compared to conventional microstrip antennas, these include: higher polarization purity, lower cross talk between adjacent antennas, easy integration to microwave integrated circuits, and broader bandwidth [2]-[3]. In addition, a ground on the same plane as the patch element offers the ability of easy integration of additional external lumped components in the design. More complexity in these antennas performance, such as phase shifting and attenuation can be achieved through added tunability.

Although the bandwidth offered is slightly higher then microstrip antennas, the coplanar waveguide antenna is still considered narrow band antenna, which is suited for limited applications only. Applications where this type of designs might find a nich are GPS, biomedical, beacons, satellite, chip-to-chip signaling and even a full identification system on a chip.

To date, no references in the literature have been observed which give analytical expressions for the design of conductor backed coplanar waveguide with finite ground planes. There are some papers on the analytical solution of conductor backed infinite waveguide, which do give expressions meaningful for design [3]-[15]. The infinite top

ground plane approximation is not valid because the antennas studied in this thesis have the ground plane smaller then the main conductor [6].

The approximation suggested here, is based on the use of three coupled transmission lines. The equations of coupled microstrip lines are readily available from numerous sources and are well established [16]-[24]. In conjunction with the above, coupled line approach, transmission line theory will be used to model the effects of radiation and thus give a more comprehensive model for the design of conductor backed coplanar waveguide patch antennas which will allow the insertion of lumped components.

2.1 Transmission Line Model

Any structure supporting wave propagation can be approximated, to a first order, as a transmission line. The coplanar waveguide patch antenna is no exception, in fact, due to the narrow bandwidth of the matching condition; the approximation in terms of equivalent transmission line model of the coplanar waveguide patch antenna is appropriate and very insightful.

The transmission line model treats the antenna as an ideal transmission line terminated in a specific load. This load takes into account the effects of edge capacitance, substrate losses, metal losses, and radiation. In a relatively thick substrate, the loads can also include the effects due to surface waves. This section will derive the basic transmission line model and will not take into account surface waves, a more detailed treatment can be found in Chapter 10 of [25].

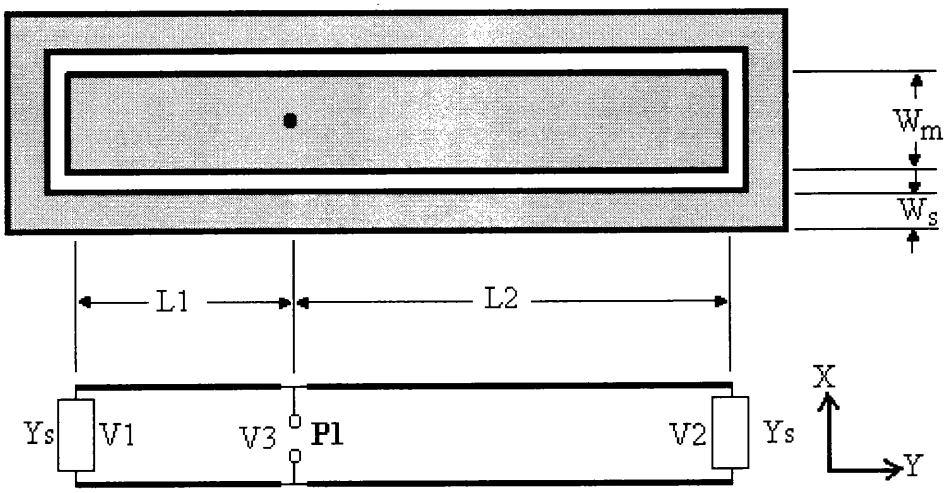

Figure 2.2.1 Transmission line equivalent to the coplanar waveguide patch antenna. Where the dark part is the metallization.

As illustrated in Figure 2.2.1, a coplanar waveguide patch antenna, in the horizontal direction, can be modeled as a pair of transmission lines, each line, with one side terminating at the feed and the other at some load. The reason for the reactance of the load is that the coplanar line does not terminate in a perfect open circuit due to the fields not stopping at the edge but extending beyond it, forming stray parasitics, specifically, of capacitive nature. The capacitive nature of the reactance can be included as an extra length of transmission line, which has to be compensated, causing the length of the physical waveguide to be more than a half wavelength. The real part of the load impedance is due to radiation and surface waves, as the transmission line itself does not account for either.

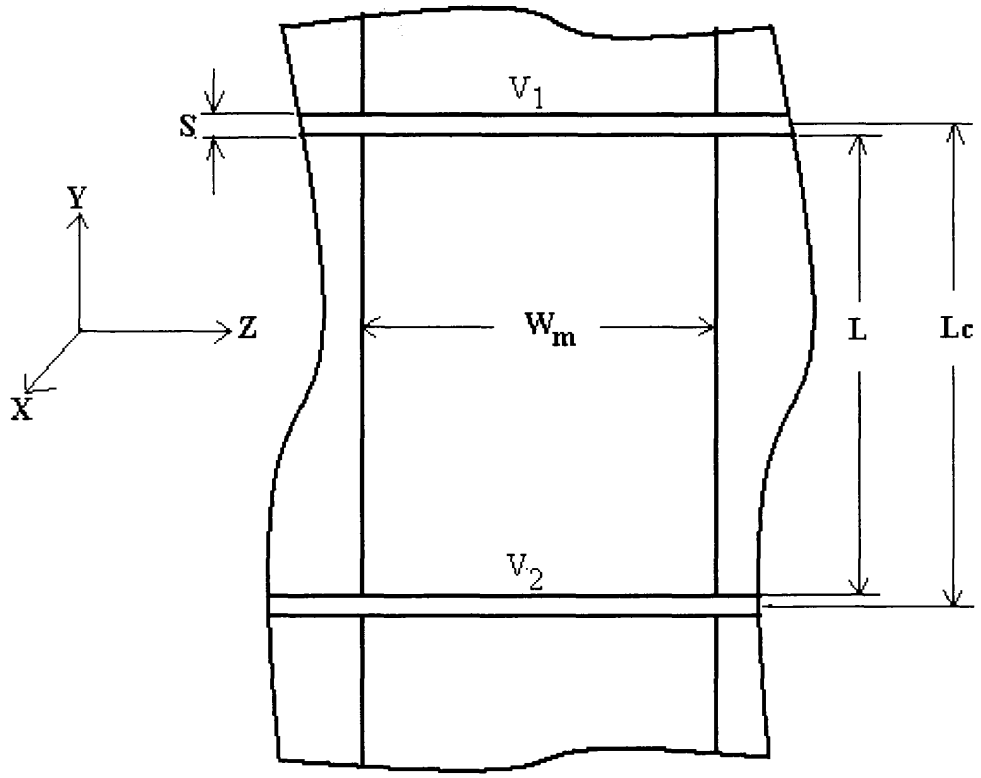

Figure 2.2.2 Infinite slot model for radiation of a coplanar waveguide patch antenna

A simplified derivation of the load impedance (as given in Chapter 10 of [23]) models the interaction at the edges of the transmission line as that of a pair of infinite slots (Figure 2.2.2). This model is valid for either very long separation of S in which the bottom ground plane interactions dominates or very short separation, in which the top ground plane effects dominates.

Starting with $Y_S = W_m y_S$, where $y_S = g_S + jb_S$ is the admittance per unit length of a uniformly excited slot of infinite length and height H of the substrate, when the ground plane dominates (S>>H), otherwise its S (S<<H). The slots length is the width of the center strip in the actual antenna. The expressions for the tangential E-field in the slot aperture are

$$E_a = \begin{cases} \frac{V_1}{S}\hat{y} & \frac{L_c - S}{2} \le y \le \frac{L_c + S}{2} \\ \frac{V_2}{S}\hat{y} & \frac{L_c - S}{2} \le -y \le \frac{L_c + S}{2} \\ 0 & Otherwise \end{cases} \qquad (2.2.1)$$

where, L_c is the center distance between the two slots, V_1 and V_2 are the excitation voltages of the two slots and S is the slot width, not necessarily the separation of the top ground plane from the center strip, as indicated above.

The Fourier transform of (2.2.1) can be defined as

$$\tilde{E}_a = \int_{-\infty}^{\infty} E_a e^{jk_y y}\, dy \qquad (2.2.2)$$

where, k_y is the $\hat{y}$ component of the propagation constant $\vec{k}$. Since the Fourier transform, $\tilde{E}_a$ has only a $\hat{y}$ component, so as E_a, leading to

$$\tilde{E}y = jS\frac{\sin(k_y S/2)}{k_y S/2}(V_1 e^{jk_y Lc/2} + V_2 e^{-jk_y Le/2})$$

(2.2.3)

substitution of (2.2.3) into the expression for the complex power (from [26] pp.61-68)

$$p = \frac{k}{4\pi\eta}\int_{-k}^{k} |Ey|^2 \frac{dk_y}{\sqrt{k_y{}^2 - k^2}} \qquad (2.2.4a)$$

and

$$q = \frac{k}{4\pi\eta}\left(\int_{k}^{+\infty} |Ey|^2 \frac{dk_y}{\sqrt{k_y{}^2 - k^2}} + \int_{-\infty}^{-k} |Ey|^2 \frac{dk_y}{\sqrt{k_y{}^2 - k^2}}\right) \qquad (2.2.4b)$$

and η is the wave impedance in the substrate. The real and imaginary parts of the power can be related to the circuit of Figure 2.2.1 to form the following equations:

$$p + jq = .5y_S^*(|V_1|^2 + |V_2|^2) + y_m^* \,\mathrm{Re}(V_1 V_2^*) \tag{2.2.5}$$

Setting V_2=0, we get the following integral equations

$$g_S = \frac{k}{\pi\eta}\int_0^k \frac{\sin 2(k_y S/2)}{(k_y S/2)2}\frac{dk_y}{\sqrt{k^2 - k_y{}^2}}$$

(2.2.6a)

and

$$b_S = \frac{k}{\pi\eta}\int_k^\infty \frac{\sin 2(k_y S/2)}{(k_y S/2)2}\frac{dk_y}{\sqrt{k^2 - k_y{}^2}}$$

(2.2.6b)

The above set of equations could be expressed as the double integrals of the Bessel function of the first kind $J_0(v)$ and second kind $Y_0(v)$ of order zero as follows

$$g_S = \frac{k}{\eta s^2}\int_0^{kS}\int_0^u J_0(v)\,dv\,du \tag{2.2.7a}$$

and

$$b_S = -\frac{k}{\eta s^2}\int_0^{kS}\int_0^u Y_0(v)\,dv\,du \tag{2.2.7b}$$

The double integrals can be expanded into series form and after, omitting terms of fourth order and higher, will simplify into

$$g_S \approx \frac{k}{2\eta}\left(1 - \frac{s^2}{24}\right) \tag{2.2.8a}$$

and

$$b_S \approx \frac{k}{\pi\eta}\left\{\left(\ln\left(\frac{s}{2}\right)+.577216-\frac{3}{2}\right)\left(1-\frac{s^2}{24}\right)+\frac{s^2}{288}\right\} \tag{2.2.8b}$$

where

$s = kS$.

The line parameters of the finite ground plane coplanar waveguide can be obtained by modeling the coplanar waveguide as the center of three coupled microstrip lines. Since the two sides are predominately grounded, the odd mode could be considered as the dominant mode, as a first order approximation.

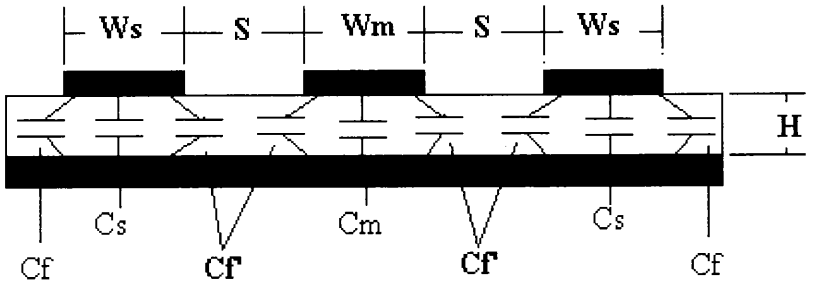

(a) even mode representation

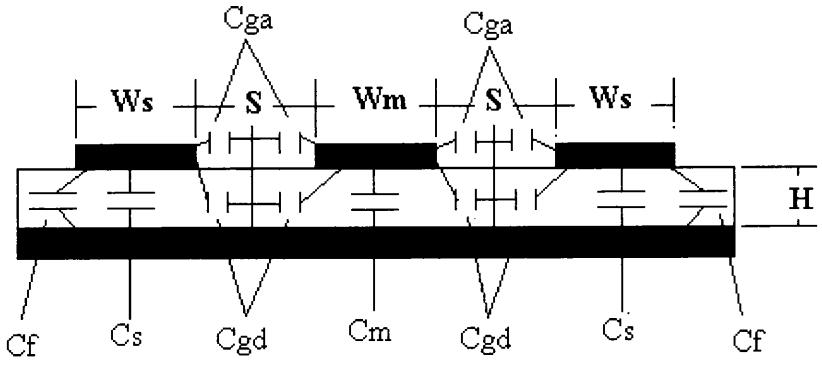

(b) odd mode representation

Figure 2.2.3 Schematic representation of three coupled microstrip lines.

The proecedures developed for two coupled lines [16] are extended to include the three line model shown in Figure 2.2.3. The odd and even mode capacitance for center and side strips can be defined as shown in Figure 2.2.3.

$$\begin{aligned} C_{me} &= 2C_{f'} + C_m \\ C_{se} &= C_f + C_{f'} + C_s \\ C_{mo} &= C_m + 2(C_{gd} + C_{ga}) \\ Cso &= C_s + C_f + C_{ga} + C_{gd} \end{aligned} \tag{2.2.9}$$

where C_{me}, C_{mo}, C_{me}, C_{se} are the even and odd center and side strip capacitors respectively, the rest of the parameters are cross coupling capacitances. These capacitances can be described in terms of physical parameters as

$$C_m = \varepsilon_0 \varepsilon_r \frac{W_m}{H} \tag{2.2.10a}$$

$$C_s = \varepsilon_0 \varepsilon_r \frac{W_s}{H} \tag{2.2.10b}$$

$$2C_f = \frac{\sqrt{\varepsilon_{re}}}{c} Z_0 - C_{m,s} \tag{2.2.11}$$

where Cm,s is the capacitance of either the middle or the side strip as defined in (2.2.9) for the associated fringe capacitance.

$$\begin{aligned} C_{f'} &= \frac{C_f}{1 + A\left(\frac{H}{S}\right)\tanh\left(12\frac{S}{H}\right)} \sqrt{\frac{\varepsilon_r}{\varepsilon_{re}}} \\ A &= e^{-.1e^{2.33 - 2.53\frac{W}{H}}} \end{aligned} \tag{2.2.12}$$

and

$$W = \frac{W_s + W_m}{2} \tag{2.2.13}$$

The capacitance associated with the slot in air is defined as

$$C_{ga} = \varepsilon_0 \frac{K(k')}{K(k)},\ k' = \sqrt{1-k^2} \tag{2.2.14}$$

and the capacitance in the substrate is given as

$$C_{gd} = \frac{\varepsilon_0 \varepsilon_r}{\pi} \ln\left\{\coth\left(\frac{\pi S}{4H}\right)\right\} + 0.65 C_f \left[\frac{.02H}{S}\sqrt{\varepsilon_r} + 1 - \varepsilon_r{}^{-2}\right] \tag{2.2.15}$$

The remaining parameters are defined as

$$\varepsilon_{effi} = \frac{C_i}{C_i{}^a} \tag{2.2.16}$$

and

$$Zi = \frac{c}{\sqrt{C_i C_i{}^a}} \tag{2.2.17}$$

The feed point is found from[31]:

$$R(y) = Z_{odd} \cos^2\left(\frac{\pi y}{L}\right) \tag{2.2.18}$$

and from [27],

$$Z_0 \sqrt{\varepsilon_{re}} = 60 \ln\left(\frac{8H}{W} - .358 + \frac{1}{0.931\left(\frac{H}{W}\right) + .736}\right) \tag{2.2.19}$$

$$\varepsilon_{re} = 1 + 0.5(\varepsilon_r - 1)\left[\left(1 + 10\frac{H}{W}\right) - .555 + 1\right] \tag{2.2.20}$$

Here, ε_{effi} and Zi are the line parameters, the subscript I referring to the even or odd component, and $C_i{}^a$ is the equivalent capacitance when $\varepsilon_{re=1}$. R(y) is the input impedance at point y along the antenna.

From equations (2.2.9)-(2.2.18), of which the results of (2.2.16) and (2.2.18) gives the line parameters which can be used with microstrip design equation to yield the length and feed point location for a particular antenna design.

CHAPTER 3

TUNABILITY

3.1 Introduction

Generally, tunability in antennas implies frequency scanning over a certain frequency band. Here, tunability will be regarded as a change in the phase of the input impedance as a function of frequency. The overall goal is to combine radiating elements and a phase shifter combination as a single tunable patch element.

The advantage of external tunable components is in their ease of mounting. Also, most devices are not suitable for integration of control devices which are commonly manufactured on Si , GaAs, or Ge. Since the devices are small in size and sealed in their own packages they often do not interfere with the radiation of the antenna or coupling in the system. Therefore, they do not need to be simulated electromagnetically as part of the antenna system. This offers the designers a system approach where each component could be treated separately thereby saving time and accuracy in numerical simulations. The disadvantage of the added external devices is their size and cost. External devices need extra room and often have separate power requirements, which could be different than from the other part of the system. In addition, there is extra cost of packaging and interconnects from such devices to the antenna elements.

Internal devices, due to their high proximity to the antenna itself, sometimes need to be taken into account electromagnetically, within the simulation, thus making them cumbersome to use. As cumbersome as they are to simulate, they do offer simple, low cost alternatives to the external modules. Even though no closed form models exist for

most cases, approximate circuit models are very good and can be used for practical design.

In the design presented here, a varactor diode is used as the tuning device. A very commonly used device in the microwave and RF arena, the varactor diode functions as a voltage tuned capacitor. A DC voltage is applied in reverse bias to the diode; as the voltage increases, the size of the depletion region increases. Since there is no charge on the depletion region, it acts as a dielectric, while the bulk region where the electric contacts are embedded act as a conductor, thus forming a capacitor like structure, which changes its capacitance inversely with the applied voltage. As the bias voltage changes so does the depletion region and thereby changing the capacitance in a very controlled way [33].

The varactor diodes are mounted on the top surface of the antenna in certain locations, where the electric field is a maximum and thus control the resonant frequency of the antenna. The diode acts as a matching element when operated over a large range and thereby significantly changing the resonance frequency of the antenna. Over a small range, dictated by the afforded impedance mismatch, the varactor diode tends to tune the phase of the antenna element. This type of approach eliminates the need of complex systems for the purpose of tunability, at least at the hardware level, and thereby allows inexpensive implementation of massive antenna arrays for low power operations, due to the capacitive change being a small signal effect. For higher power applications, ferroelectric tuning elements are attractive alternatives.

3.2 Implementation

Using the transmission line method introduced in Section 2.2, a varactor diode is added as a tuning element in a planar waveguide patch antenna. The diode, with an appropriate DC offset, acts as a capacitor applied on the line, the location in the electric model being directly related to the position in the physical structure. Therefore, the effect can be predicted very accurately, and optimization can be made utilizing ordinary circuit simulators instead of field simulators, provided that the effects of the component's package are negligible.

The circuit model of a tuning element has also to include the packaging effects. Therefore, only a circuit model would not give an accurate representation but it would give a good intuitive understanding. In addition, just adding a capacitor does not induce great change because the phase shift due to a capacitor is a constant 90 degrees. In order to provide a variable phase shift, a more complex circuit is needed. The circuit employed in the various experiments conducted here, is a parallel tank circuit.

The reasoning for using a parallel tank as oppose to a series tank circuit is that at resonance the impedance is very high and therefore should not disturb greatly the original operation of the antenna. When the lump circuit moves out of resonance its reactance becomes either inductive or capacitive and thereby changing the characteristic of the antenna by appearing to either shorten its length or increase it.

This apparent change of length also changes the impedance match of the antenna to the load impedance, for small changes in capacitance, the input impedance of the antenna does not change much but its phase changes more significantly.

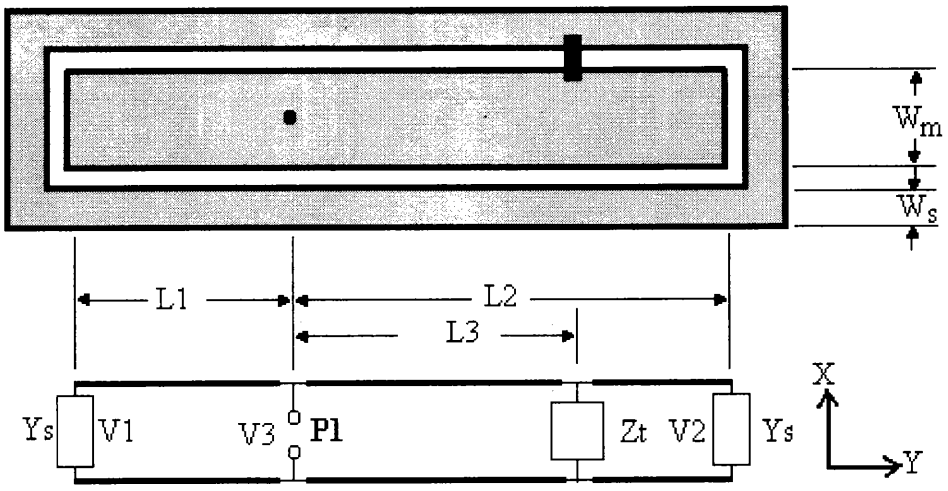

Figure 3.2.1 Transmission Line model with lumped tuning element. The dark part is metallization.

Figure 3.2.1 shows one possible configuration used for the tuning element. The element can be placed on many locations along the line as well as multiple elements can be used. The planar transmission line configuration allows ease of element placement since the element can remain in the same plane provided the spacing between the center conductor and the ground plane is small enough to accommodate the element placement.

CHAPTER 4

SIMULATIONS AND EXPERIMENTAL RESULTS

The following procedure was followed to construct the antennas. First the size of the antenna was estimated using analytical approximations. These results served as initial values for further optimization using the IE3D software tool. Once the desired input impedance is obtained within 1% or better tolerance level, the geometry would be optimized further by the simulator's Genetic Algorithm search procedure.

Once the desired optimization limits are achieved, the obtained result for the antenna geometry was drawn on a CAD drawing program, adding 1/32 of an inch for etching margin, and printed on an thermal-transfer paper. The paper would then be placed on the cut printed circuit board and heat transferred over to the copper. Covering the back ground plane with duct-tape in order to prevent etching and retouching the top ground plane and center conductor with whiteout and permanent marker, the board is then placed in FeCl solution to be etched.

Once the etching is completed, the board is drilled at the feed location and the coaxial-feed probe is soldered in place. Care must be taken so that the center conductor of the feed does not make contact with the back ground plane.

After placing the feed, the antenna is then measured with the HP8510C vector network analyzer and tuned to have the input impedance of the antenna close to a 50 ohm match at the desired frequency. This, however, cannot be achieved exactly and therefore an S11 parameter of –20 to –30 dB is considered as an acceptable value.

The varactor diode is then mounted on a tuned antenna in the location determined by simulation and reconnected to the calibrated network analyzer through a DC block. A DC voltage is applied to the antenna to bias the varactor diode and the network analyzer measures the antenna response. The result is then stored on a disk and read by a spreadsheet for processing.

Figures 4.1-4.7 show the results obtained for antennas heaving two different type of substrate. The location of the diode was optimized for maximum phase shift by changing the placement location on the patch geometry and the location with the biggest phase change response was selected using IE3D software.

As seen from comparing the response of the simulation, there is noticeable difference in operating frequency of the antenna. This is mostly due to the diode enclosure not taken into account because when the structure was tuned without the diode, it was tuned to the simulated resonance. Another cause of such discrepancy is the bias line which is added during measurements but was not included in simulation. The observed experimental trend, however, is very similar, and does show a reasonable amount of phase shift for different bias voltage values.

Figure 4.1 depicts the magnitude and phase of scattering coefficient S_{11} from a conductor backed coplanar waveguide antenna with one tuning varactor diode. The experimental results show a significant amount of phase shift of approximately 60 degrees around the resonance frequency of 1.2 GHz. The theoretical results show a similar trend around 1.03GHz. The shift in frequency from the experimental and the theoretical values is most likely due to the effect of the biasing wires.

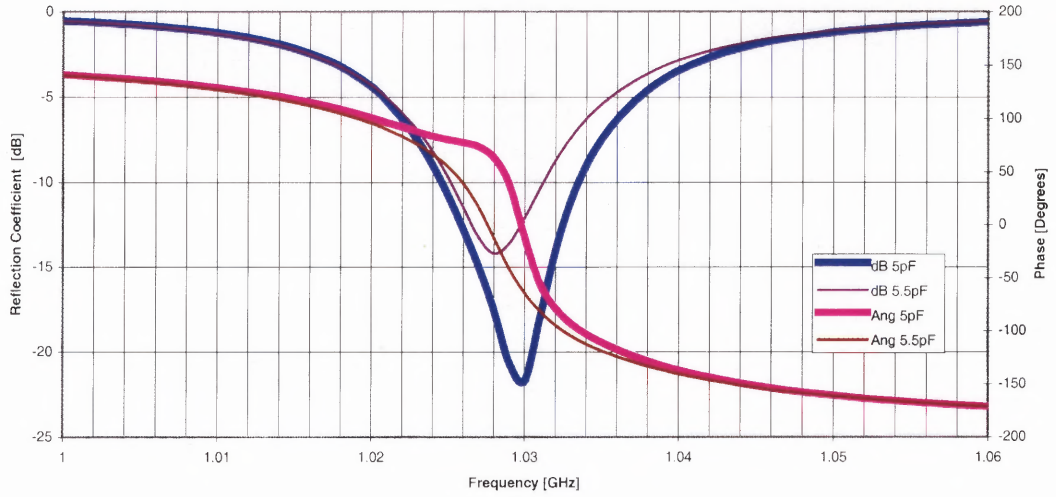

(a) Simulated input reflection coefficient and phase

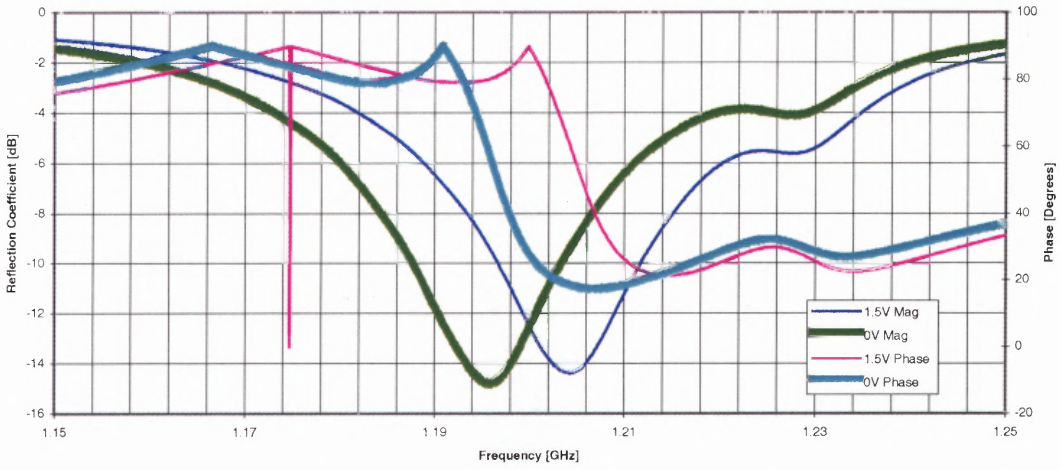

(b) Experimental input reflection coefficient and phase

Figure 4.1 Numerical and Experimental results Wm=2.597", L=2.587" Ws=1/4", S = 1/16" , h=92mill $\varepsilon_r = 4.85$ substrate and one diode.

Figure 4.2 and 4.3 are the experimental and the theoretical curves, respectively, have a two diode tuned antenna similar to the one presented in figure 4.1 The tuning diodes are placed on opposite sides of the antenna. The phase shift was not as significant for this orientation as it was for the one-diode configuration. This is due to the diodes being on opposite sides and therefore one could tend to cancel the effect of the other.

Figure 4.4 shows a patch antenna that was not attempted experimentally but it was simulated. The simulated results show a remarkable amount of phase shift but at a huge penalty in the amplitude, therefore this configuration is considered as not optimal and experimental verification was not pursued.

Figure 4.5 corresponds to experimental response of an antenna on a thicker substrate that was optimized for 2.5GHz. At 2.44 GHz, which is the experimental peak, there is about 50 Degrees phase shift with a large penalty in the amplitude, which translates to poor impedance matching. This choice of a thicker substrate was to see the tuning performance for a wider band antenna.

Figure 4.6 corresponds to a simulated average current density on the patch. It can be seen that, as predicted by (2.2.18) the patch has the highest current density at the center, corresponding to low input impedance and low current density along the width at the edges corresponding to high impedance. The sides along the length have a high current density and are considered as equivalent short circuits.

Figure 4.7 depicts the radiation pattern from the patch, of Figure 4.5, indicating little or no surface waves and also little effect on the pattern from the diode or the coplanar waveguide as compared to a microstrip patch. The simulated radiation efficiency is determined around 75%.

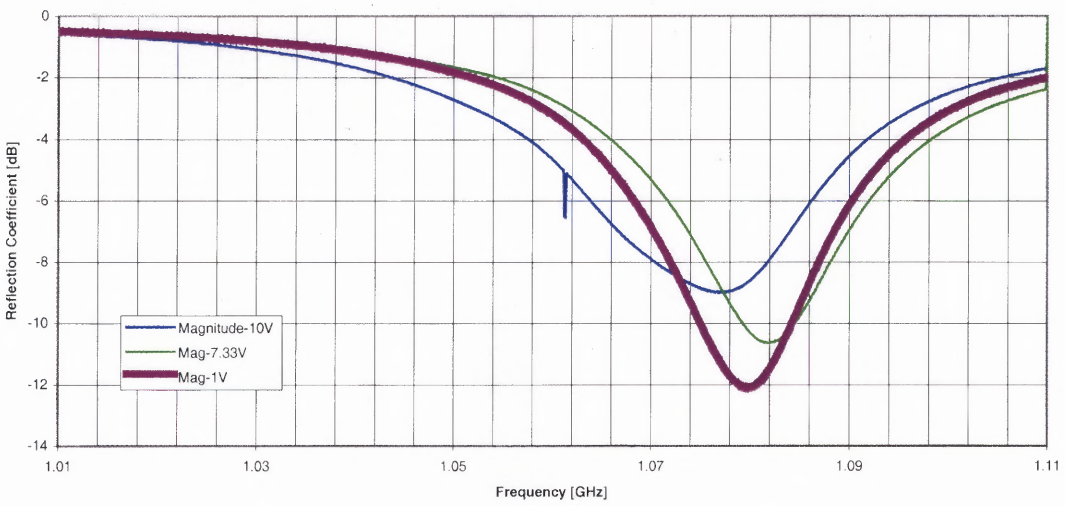

(a) Experimental reflection coefficient

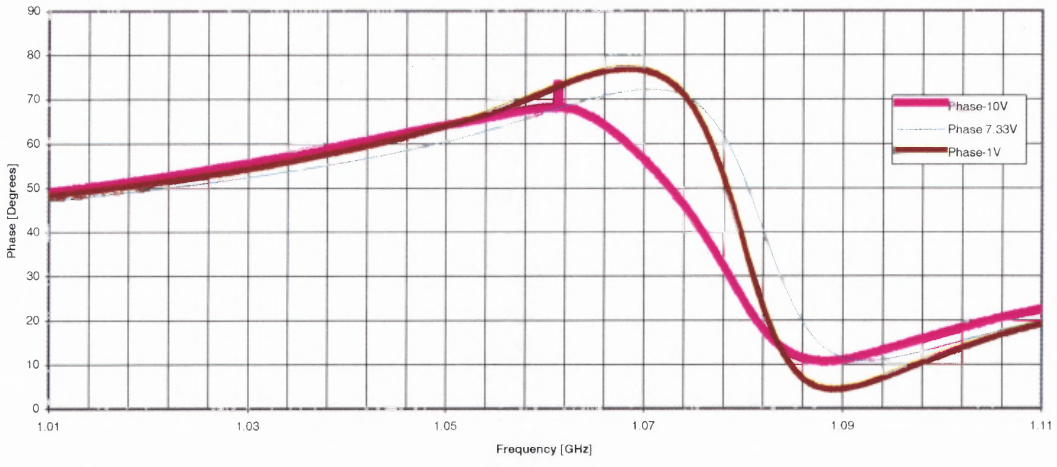

(b) Experimental Phase

Figure 4.2 Experimental results Wm=2.597", L=2.587" Ws=1/4", S =1/16" , h=92mill $\varepsilon_r = 4.85$ substrate and two diodes.

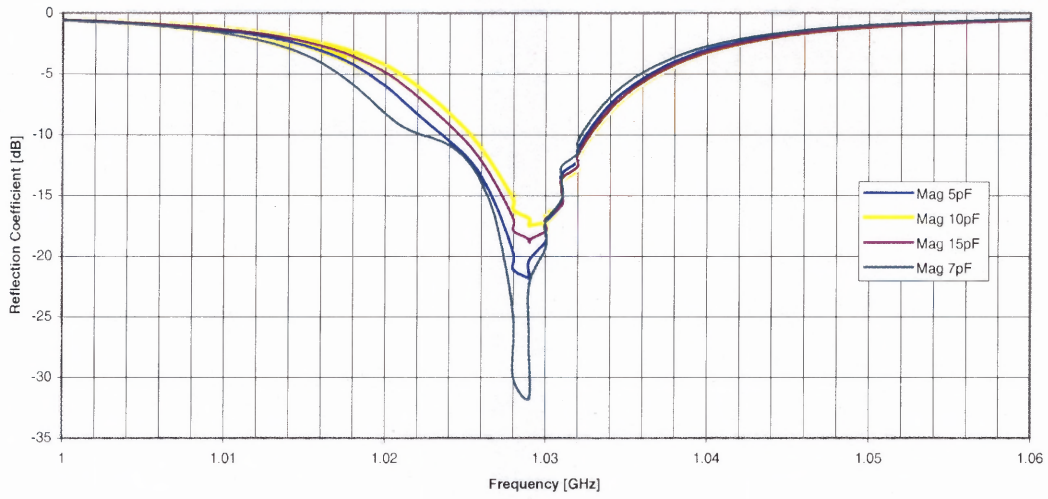

(a) Reflection coefficient

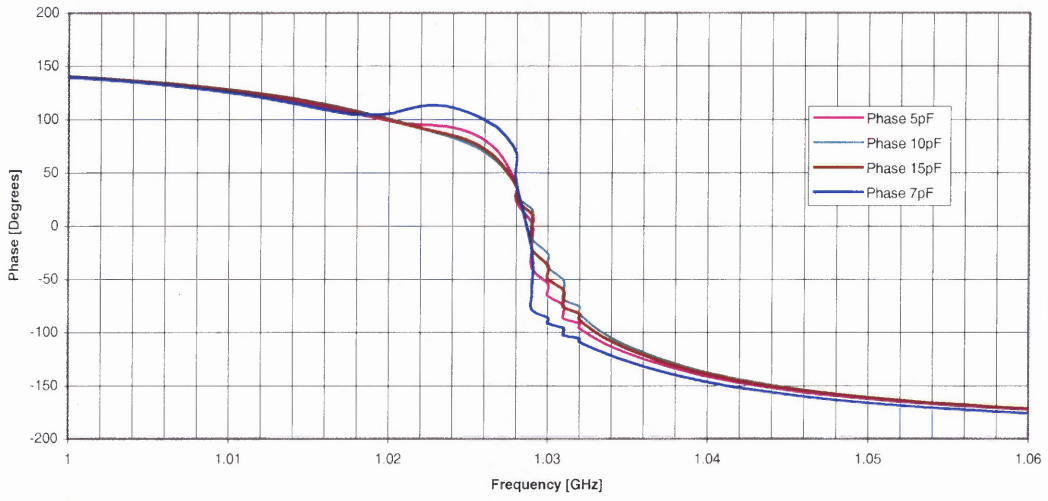

(b) Phase

Figure 4.3 Simulated results Wm=2.597", L=2.587" Ws=1/4", S =1/16" , h=92mill $\varepsilon_r = 4.85$ substrate and two diodes.

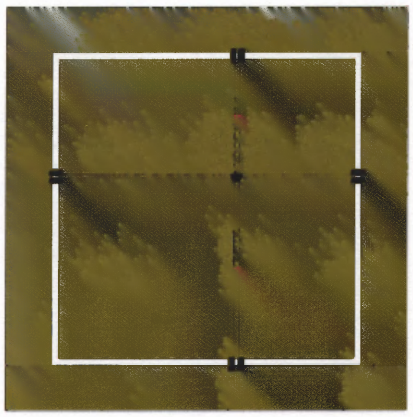

(a) Patch Antenna with four tuning elements

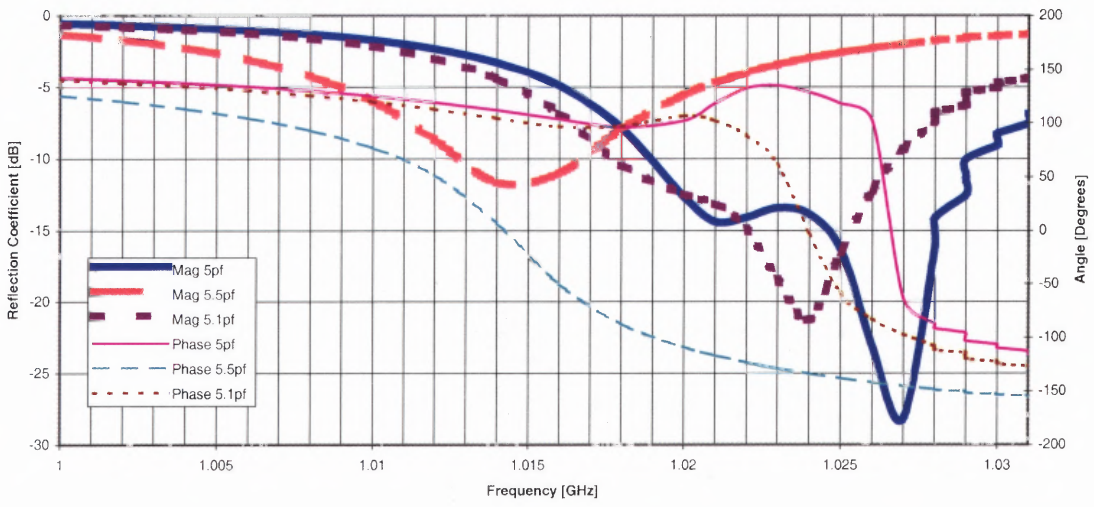

(b) Simulated Results

Figure 4.4 Simulated results for Wm=2.597", L=2.587" Ws=1/4", S = 1/16" , h=92mill $\varepsilon_r = 4.85$ and four varactior diode.

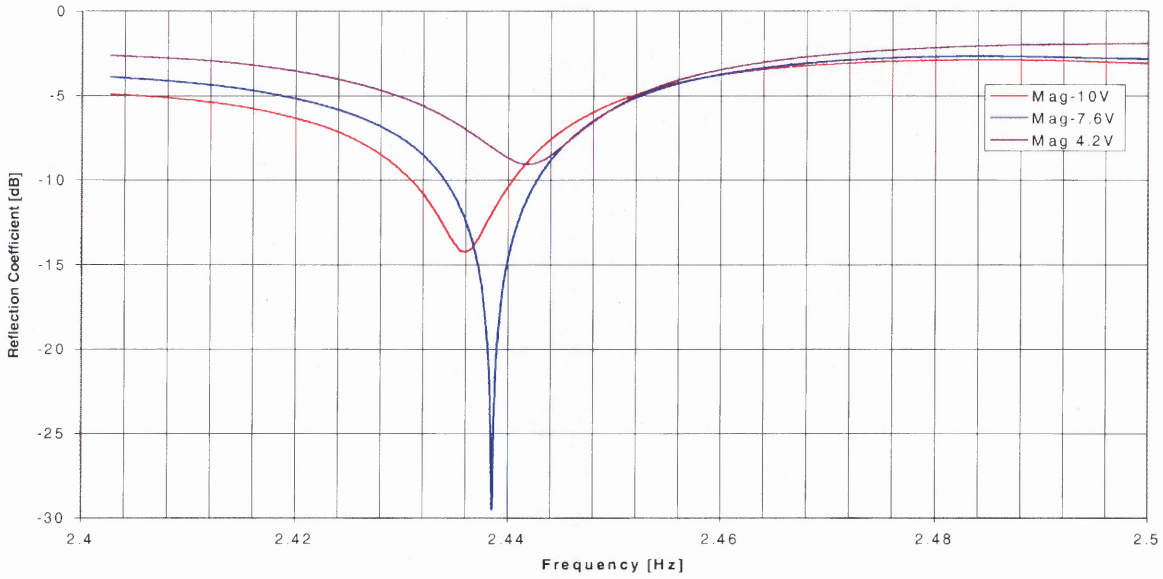

(a) Reflection Coefficient

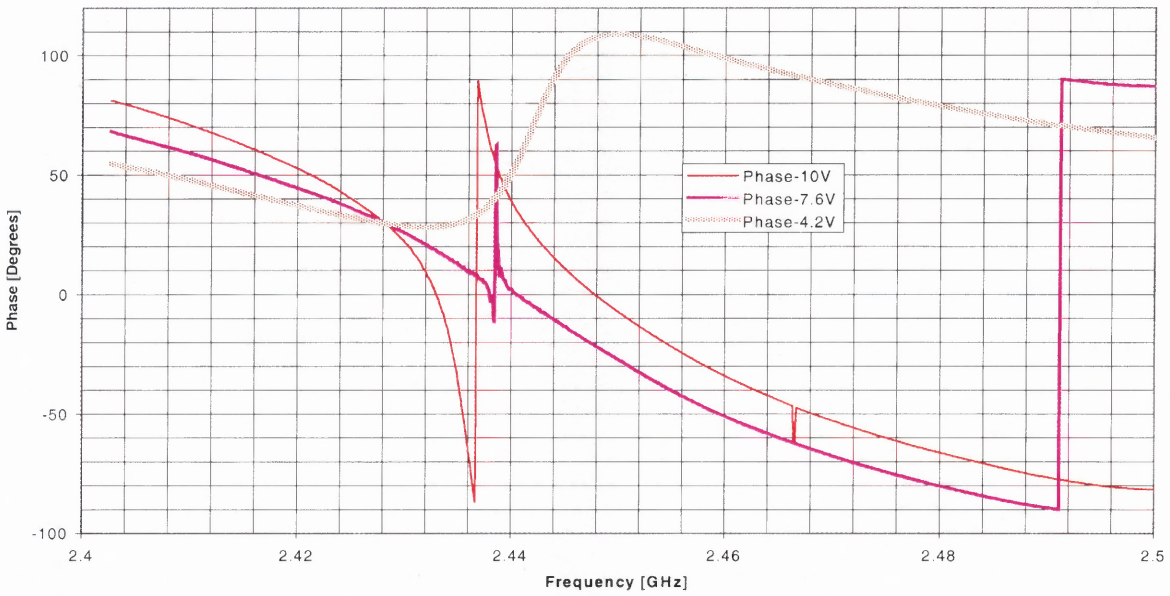

(b) Phase

Figure 4.5 Experimental Wm=2.597", L=2.587" Ws=.5", S = .1" , h=250mill $\varepsilon_r = 4.85$ and one varactor diode.

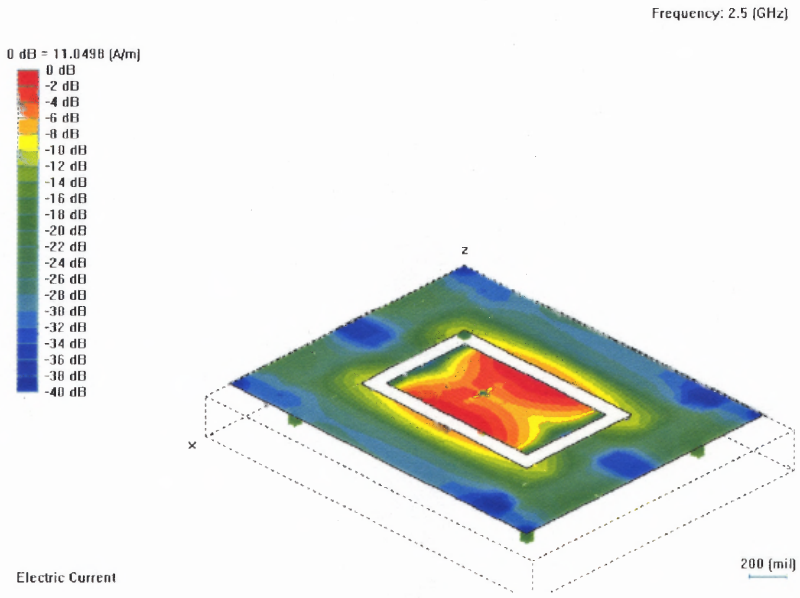

Figure 4.6 Average Current Density of the antenna constructed in Figure 4.5

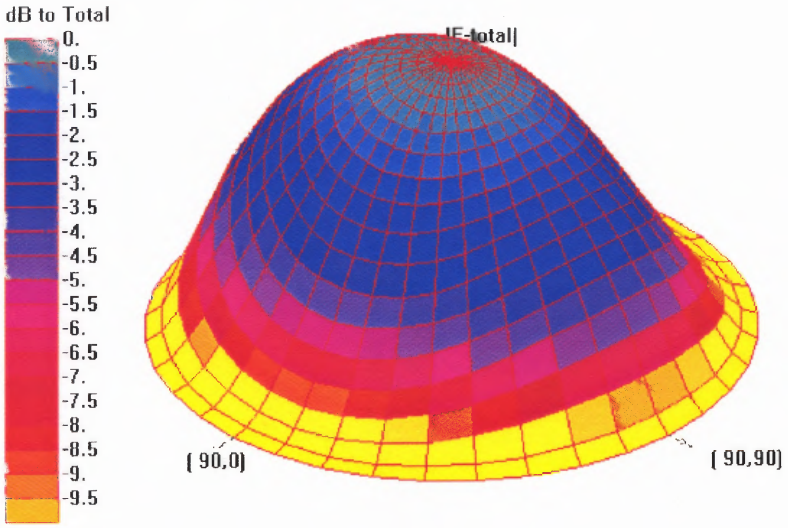

Figure 4.7 A 3-D Antenna Pattern Generated by IE3D for the antenna in Figure 4.5

These results confirmed experimentally that tunability in antennas introduced significant phase change in a relatively narrow frequency band where the antenna maintains low input VSWR. Due to a finite Q of the tuning elements, additional loss is introduced.

CHAPTER 5

CONCLUSION

In this thesis, a novel application of a tunable antenna is suggested as an attractive alternative for a combination of a radiating element and a phase shifter. This concept has been implemented on a conductor backed coplanar waveguide patch antenna due to its suitability to surface mount external tuning elements. Due to limited time, tuning approach was based on varactor diodes and inductors only, but the chosen antenna geometry is very suitable for ferroelectric as well as distributed tuning along the perimeter of the patch.

Here, approximate analytical models for the coplanar waveguide patch antenna with finite ground plane, were developed. These models were effectively used to determine approximate dimensions of the patch and the feed location for the given size of the ground plane and the slot width. Using initial results based on these approximate methods in the commercially available IE3D software, faster convergence of optimal results have been achieved.

Based on the simulations, antennas were constructed and manually optimized further to the specified operating frequency band. Then tuning elements were mounted. Experimental characterization of the tunable antennas was carried out. As bias voltage is introduced for tuning, slight increase of loss and incremental shift in frequency were obtained. However, the phase of the reflection coefficient at the feed point showed significant shift for variation in the bias voltage. The higher the Q of the tuning circuitry, the less will be changes in the return loss. Despite all the losses, variation of the phase

within a certain band are equally acceptable as a potential phase shifter for the antenna. Distributed tuning seems to be a very attractive option to achieve even higher phase shift.

Though a microstrip patch and a conductor backed coplanar waveguide patch antenna exhibit narrow bandwidths, initial measurements that were not reported in the thesis favor the latter one in terms of wider bandwidth response. Further research could be in evaluation of distributed tuning along the slot as well as usage of exotic ferroelectric and magnetic materials.

APPENDIX A

METHOD OF MOMENTS

A.1 Method of Moments Formulation

In order to accurately characterize the planar antenna, the current distribution has to be determined through solutions of Maxwell's equations with proper boundary conditions. The planar antenna does not lend itself to a closed form analytical solution; therefore in order to achieve a solution, one has to resort to numerical methods. Numerical solutions can be obtained from integral equation formulation for the unknown current distributions.

The generalized problem of this nature can be represented as

$$L(f) = g \tag{A.1.1}$$

where L is defined as a linear operator that is known, g is a source, or excitation function that is also known, and f is the response to be determined.

Following [29], The method of moments formulation attempts to solve (A.1.1) by taking f and expanding it into multiple functions f_n:

$$f = \sum_n \alpha_n f_n \tag{A.1.2}$$

and therefore:

$$\sum_n \alpha_n L(f_n) = g \tag{A.1.3}$$

The functions, f_n, are called basis functions, which together with their coefficients α_n give an approximate solution to the problem, unless the basis form a complete set, in which case the solution is complete.

Some of the more common functions used for the basis are the pulse and triangular functions. The pulse function is defined as

$$P(\xi) = \begin{cases} 1 & |\xi| < 1 \\ 0 & Otherwise \end{cases} \tag{A.1.4}$$

and the triangular function is defined as

$$T(\xi) = \begin{cases} 1 - |\xi| & |\xi| < 1 \\ 0 & Otherwise \end{cases} \tag{A.1.5}$$

The triangle function provides a smoother transition and sometimes better approximation. The functions (B.1.4) and (B.1.5), in addition to provide a means of approximation for the response, also provide a mean of discretizing the response, since they are zero in all but a relatively small area.

If one thinks about dividing the geometry into many small sections, as shown in Figure B.1.1a, one can overlap the basis functions, above, and by superposition of the bases multiplied by their coefficients one can form a myriads of desired functions (Figure B.1.1b-c.)

Since an approximation is made, it might be desired that certain parts of f, be more importance then others, which sometimes helps to increase convergence. This can be done by introduce a weighting function w_m, where m=1,2,3… :

$$\sum_n \alpha_n < w_m, L(f_n) >=< w_m, g > \tag{A.1.6}$$

$$< f, g >=< g, f > \quad (Commutative\ \Pr operty) \tag{A.1.4a}$$

$$< af + bf, g >= a < f, g > + b < f, g > \quad (Linearity\ \Pr operty) \tag{A.1.4b}$$

$$< f^*, f >> 0 \ \ if\ f \neq 0 \tag{A.1.4c}$$

$$< f^*, f >= 0 \ if\ f = 0 \tag{A.1.4d}$$

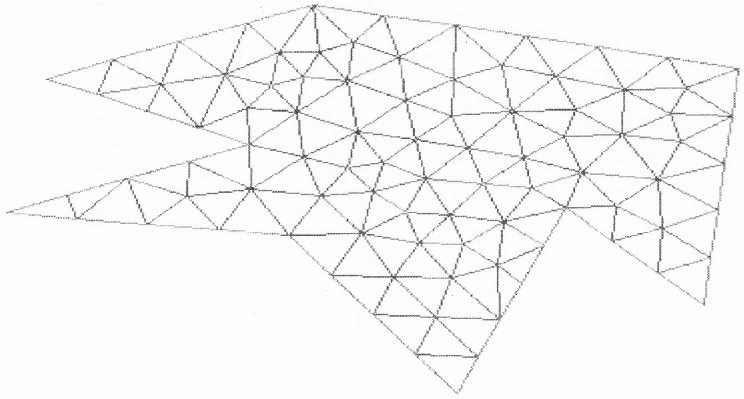

(a) The division of a structure into cells.

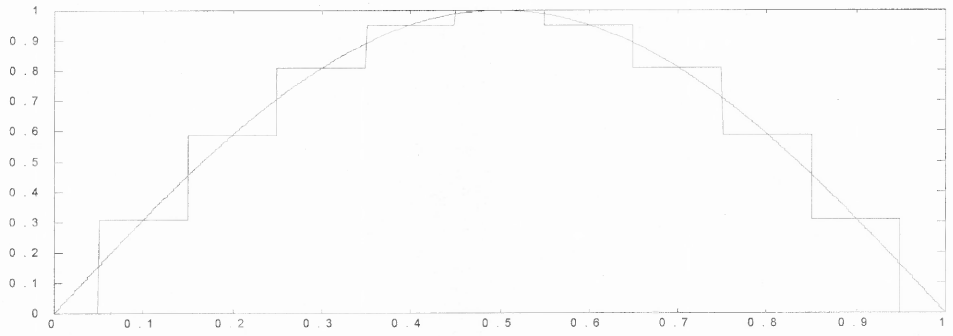

(b) The approximation of a function by rectangular basis functions.

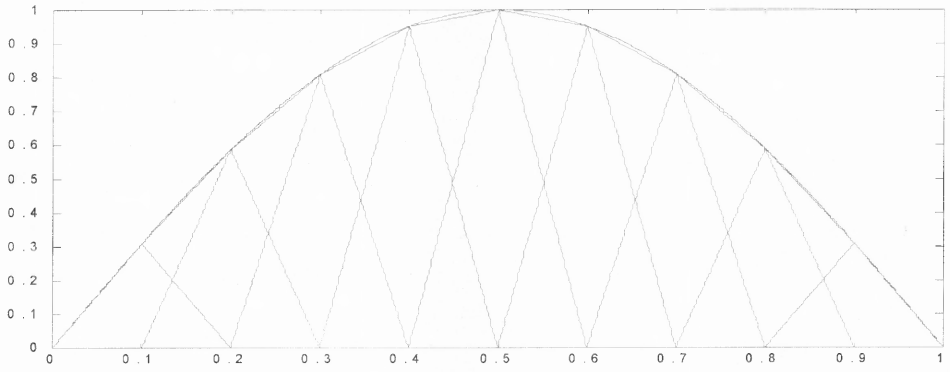

(c) The approximation of a function by pulse basis functions.

Figure A.1.1

Where <[],[]> is a suitable functional inner product (B.1.4) which leads to systematic approach, commonly known as Method of Moments. Likely, weighting functions can be delta functions, in which case the method is called the point matching method or they can be the basis functions themselves in which case the method is referred to as the Galerkin method. The point matching method is a very commonly used, due to the delta weighting functions, since they eliminate a lot of evaluations when taking the inner product, making some problems solvable that would otherwise be impractical, achievable with a relatively short amount of effort. One note of caution, if delta functions are chosen, then they must not correspond to a discontinuity in the basis function, for example, they must not be applied on the peak of the triangular basis function.

Equation (B.1.3) can be written in matrix form

$$[l_{mn}][\alpha_n] = [g_m] \tag{A.1.5}$$

Where, $l_{mn} =< w_m, L(f_n) >$ and $g_m =< w_m, g >$. Once $[l_{mn}]$ is found, $[\alpha_n]$ can be found by taking the inverse of the matrix $[l_{mn}]$ and thus

$$[l_{mn}]^{-1}[g_m] = [\alpha_n] \tag{A.1.6}$$

The coplanar microstrip antenna problem can be formulated in a similar approach described above leading to a solution using the Method of Moments, with the appropriate boundary conditions specified as:

$$Z_S(r)J(r) = E_i(r) + \iint_S G(r,r') \bullet J(r')ds' \tag{A.1.7}$$

where $Z_S(r)$ is the surface resistivity, $J(r)$ is the current density vector, $E_i(r)$ is the incident electric field, $G(r,r')$ is the appropriate dyadic Green's function, r is an

observation location where the field is known, r' is a source location where the current is to be determined. Comparing (B.1.7) with the previous discussion, the elements can be identified as follows: $J(r')$ is the response to be determined, $E_i(r)$ is the source term. Breaking up $J(r')$ into a summation of basis $J(r') = \sum_n I_n B_n(r')$ and applying Gauss' law, (B.1.7) can now be transformed into the form of (2.4.5) as follows (applying the Galerkin's method):

$$[Z_{mn}][I_m] = [V_m] \tag{A.1.8}$$

where,

$$Z_{mn} = \iint_S (Z_S(r) B_m(r) \bullet B_n(r)) ds + \iint_S ds \iint_S ds' B_m(r) \bullet G(r, r') \bullet B_n(r') \tag{A.1.9}$$

and

$$V_m = \iint_S E_i(r) \bullet B_n(r) ds \tag{A.1.10}$$

The Green's function to be used for the planar antenna is that of a horizontal dipole in a stratified media (Appendix B.)

There was no need to implement Method of Moments using numerical code due to availability of commercial software tools.

B.2 IE3D Software

Many Method of Moments programs utilize a process very similar to the above. One such commercial program, utilized in this research is IE3D (Integral Equations in Three Dimensions) by Zealand Software. IE3D is a generalized full wave integral equation method of moments program to solve any type of metalized planar circuit in three dimensions. In addition, once the currents are found, the near-field and far-field

patterns can also be found. The real strength of the program is its optimization routine, allowing the user to utilize rough approximate dimensions, like ones from the method in section 2.2 and through the optimization routine approach a matched solution based on port parameter criteria. The program also allows the calculation of an array of similar elements with different spacing and feed phases.

The shape of the structure, as well as layer information is entered through a conventional designed interface. Once in place, the user selects the simulation parameters, such as frequency and grid size. The simulation is then executed and the results displayed in a form of a smith chart or any other mean.

One of the strengths of this particular package is that it enables lumped component functionality, in which external components can be placed at ports and the structure could be simulated. Once done, the effects of the components on the fields can be shown graphically. This is in contrast to using the S parameter output of the simulation and thereby only using the 'dead' network to view the results at the ports and not the overall field and current distribution.

APPENDIX B

GREEN'S FUNCTION OF A HERTZIAN DIPOLE

IN A GROUNDED SUBSTRATE

Following the derivation of [32]:

The expression for the electric field, in terms of the Green's function and current distribution is

$$E_x(x,y) = \iint G_{xx} J_x(x_s, y_s) dy_s dx_s + \iint G_{xy} J_y(x_s, y_s) dy_s dx_s \tag{B.1}$$

and

$$E_y(x,y) = \iint G_{yx} J_x(x_s, y_s) dy_s dx_s + \iint G_{yy} J_y(x_s, y_s) dy_s dx_s \tag{B.2}$$

where $G_{xx}, G_{yx}, G_{xy}, G_{yy}$ are the spatial-domain dyadic Green's functions which can be obtained by taking the inverse Fourier transform of the spectral-domain Green's functions as follows

$$G_{ij}(x,y;xs,ys) = \frac{1}{r_0} \iint \widetilde{G}_{ij}(k_x, k_y) e^{-jk_x(x-xs)} e^{-jk_y(y-ys)} dk_x dk_y \tag{B.3}$$

where i and j are either x or y and $\widetilde{G}_{ij}$ is the spectral domain Green's function given as follows

$$\widetilde{G}_{xx}(k_x, k_y) = \frac{1}{\varepsilon_2} \left[\frac{k_0^2 n_2^2 - k_x^2}{D_e(k)} A_1(k) - \frac{k_x^2}{D_e(k) D_m(k)} B_1(k) \right] \tag{B.4a}$$

and

$$\widetilde{G}_{yy}(k_x, k_y) = \frac{1}{\varepsilon_2} \left[\frac{k_0^2 n_2^2 - k_y^2}{D_e(k)} A_1(k) - \frac{k_y^2}{D_e(k) D_m(k)} B_1(k) \right] \tag{B.4b}$$

and

$$\widetilde{G}_{xy}(k_x,k_y)=\frac{-k_xk_y}{\varepsilon_2}\left[\frac{A_1(k)}{D_e(k)}+\frac{B_1(k)}{D_e(k)D_m(k)}\right]=\widetilde{G}_{yx}(k_x,k_y) \tag{B.4c}$$

where

$$D_e(k)=q_2\left(q\sinh q_1b+\frac{q_1}{\mu_1}\cosh q_1b\right)\cosh q_2(h-b)+ q_2\left(\frac{q_2}{\mu_2}\sinh q_1b+\frac{\mu_2qq_1}{\mu_1q_2}\cosh q_1b\right)\sinh q_2(h-b) \tag{B.5a}$$

and

$$D_m(k)=\frac{q_2n_2^2}{\mu_2}\left(q_1\mu_1\sinh q_1b+qn_1^2\cosh q_1b\right)\cosh q_2(h-b)+ \left(q_2^2n_1^2\cosh q_1b+\frac{n_2^4\mu_1qq_1}{\mu_2^2}\sinh q_1b\right)\sinh q_2(h-b) \tag{B.5b}$$

and (B.5c)

$$A_1(k)=\left[\frac{q_1}{\mu_1}\sinh q_1b\cosh q_2(h-z_S)+\frac{\mu_2qq_1}{\mu_1q_2}\cosh q_1b\sinh q_2(h-z_S)\right]\sinh q_2(z_s-b)+ \left[\left(q\sinh q_2(h-z_s)+\frac{q_2}{\mu_2}\cosh q_2(h-z_s)\right)\sinh q_1b\cosh q_2(z_s-b)\right]\sinh q_1b\cosh q_2(z_s-b)$$

And (B.5c)

$$B_1(k)=q_2\left\{\left(n_2^2-n_1^2\right)\left[\left(q\sinh q_2(h-z_s)+\frac{q_2}{\mu_2}\cosh q_2(h-z_s)\right)\left(\frac{qn_2^2}{\mu_2}\cosh q_2(h-z_s)+ q_2\sinh q_2(h-z_s)\right)\sinh q_1b\cosh q_1b-\left(1-n_2^2\right)\left[\frac{q_1}{\mu_1}\cosh q_1b\sinh q_2(z_s-b)+ \frac{q_2}{\mu_2}\sinh q_1b\cosh q_2(z_s-b)\right]\left[q_2n_1^2\cosh q_1b\sinh q_2(z_s-b)+ \frac{\mu_1q_1n_2^2}{\mu_2}\sinh q_1b\cosh q_2(z_s-b)\right]\right\}$$

in which

$$k = \sqrt{k_x^2 + k_y^2} \tag{B.6a}$$

$$q = \sqrt{k^2 - k_0^2} \tag{B.6b}$$

$$q_1 = \sqrt{k^2 - k_1^2} \tag{B.6c}$$

$$q_2 = \sqrt{k^2 - k_2^2} \tag{B.6d}$$

$$n_1 = \sqrt{\mu_1 \varepsilon_1} \tag{B.6e}$$

$$n_2 = \sqrt{\mu_2 \varepsilon_2} \tag{B.6f}$$

$$k_0 = \omega \sqrt{\mu_0 \varepsilon_0} \tag{B.6g}$$

$$k_1 = k_0 n_1 \tag{B.6h}$$

$$k_2 = k_0 n_2 \tag{B.6i}$$

APPENDIX C

ANTENNA PARAMETERS

C.1 Parameter Definitions

There are several parameters, which are commonly used to describe the performance criteria of an antenna or an array of antenna elements. The antenna engineer's goal is to realize the design that meets those specifications. These parameters, such as: Gain, Input Impedance, Bandwidth, Beam Width, etc… will be defined in this section.

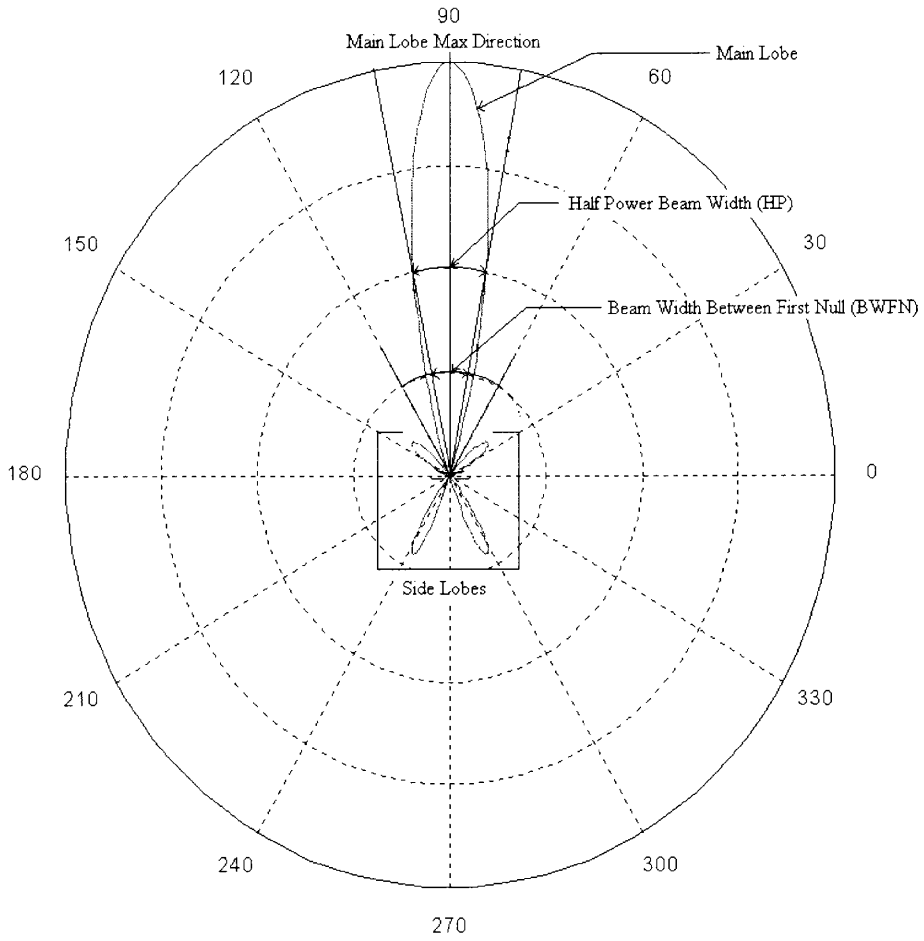

Figure C.1.1 A typical antenna radiation pattern

Figure C.1.1 shows a typical far field radiation pattern from an antenna. It has all the components that could be used to describe the beam. The radiation pattern is typically plotted in polar or rectangular coordinates. In polar coordinates, the angle represents the angular position, at a given radius, which is usually in the far field, around a fixed point in the antenna; the r-axis represents the intensity measured. In rectangular coordinates, the x-axis is usually the angle and the y-axis is the intensity. The graphs are usually in the logarithmic units of Decibels.

The pattern displayed in the polar graph may consist of a number of lobes. The lobe with the largest radius is considered as the main lobe. The lobes directly in back of it are called the back lobes and the ones to the side are called side lobes. The radiation pattern may be represented by a number of different methods, one of which is a cross section, as represented by Figure C.1.1, another is a 3-D plot, and many other exist. The usual notation [28] to represent the plotted matter is usually given in spherical coordinates and, convention has it, is given by $F(\theta,\phi)$ or $P(\theta,\phi)$ for power.

A couple of other definitions are associated with the radiation pattern they will be defined next. The side lobe level is the amount of power concentrated at the side lobe compared to the main lobe and is defined as

$$SLL_{dB} = 20Log_{10}\left|\frac{F(SLL)}{F(MAX)}\right| \qquad \text{(C.1.1)}$$

where, $F(SLL)$ is the maximum side lobe level and $F(MAX)$ is the maximum level at the main lobe.

The width of the main lobe is usually indicated in a quantity called half power beam width (HP) which is defined in a plane containing the direction of the maximum of a beam, the angle between the two directions in which the radiation intensity is one-half (-3dB) of its maximum value.

An auxiliary quantity, often used to evaluate directivity and also gain is called the radiation intensity

$$U(\theta,\phi) = \tfrac{1}{2}\mathrm{Re}\left\{\vec{E}\times\vec{H}^*\right\}\cdot r^2\hat{r} = U_m\left|F(\theta,\phi)\right|^2 \tag{C.1.2}$$

where $U(\theta,\phi)$ is the radiation intensity, $\vec{E}$ is the electric field vector and $\vec{H}^*$ is the conjugate of the magnetic field vector. U_m is the maximum radiation intensity.

The average radiation intensity can be defined as the integral of the radiation intensity over the solid angle Ω, which is also related to the total power P as follows

$$U_{avg} = \frac{1}{4\pi}\oiint_S U(\theta,\phi)d\Omega = \frac{P}{4\pi} \tag{C.1.3}$$

Directivity is now defined as the proportion of radiation intensity in a given direction to the average radiation intensity

$$D(\theta,\phi) = \frac{U(\theta,\phi)}{U_{avg}} = \frac{4\pi}{\Omega_A}\left|F(\theta,\phi)\right|^2 \tag{C.1.4}$$

and

$$\Omega_A = \iint\left|F(\theta,\phi)\right|^2 d\Omega \tag{C.1.5}$$

Maximum directivity is then given as

$$D = \frac{U_m}{U_{avg}} = \frac{4\pi}{\Omega_A} \tag{C.1.6}$$

A quantity similar to directivity but conveys a real practical meaning is called the power gain of the antenna. The power gain is a measure of how efficient the antenna is as a radiator, as it is a ratio of the radiation intensity to the input power

$$G(\theta,\phi) = \frac{4\pi U(\theta,\phi)}{P_{in}} = \frac{e_r U(\theta,\phi)}{U_{avg}} \qquad \text{(C.1.7)}$$

where e_r is the efficiency or the proportion of power radiated to the input power. Another related quantity is the maximum gain, which is defined similar to the maximum directivity: $G = e_r D$, where G is the maximum gain and D is the maximum directivity.

A quantity, which is related directly to the spacial behavior of the antenna radiation and its orientation, is the antenna polarization state. There are four main polarization states, others are just a super position of those four[1], a visual description is shown in Figure C.1.1

An antenna, just like any other device can be translated into an electric network. For the purposes of this section, the antenna will be viewed as a one port network. If one looks into that port, which shall be designated as port 1, there will be an impedance which will consist of a real and imaginary parts Z=R+jX, where the reactance, X, conveys the energy stored in the near field of the antenna and the resistive component conveys the power lost due to ohmic losses and radiation losses. In an antenna design the desire is to maximize the radiative power and minimize the stored and ohmic losses.

The impedance of an antenna can be viewed in another, more intuitive way. The one port network can be described in terms of its scattering parameters matrix. Power going into port 1 can either continue into the antenna or reflect back. If power reflects

[1] The circulars can be decomposed to a combination of linear and vice versa, so in essence you only need two.

back, that power is not radiated. The power that goes into the port either gets absorbed or radiated but it is not possible to differentiate the absorbed and radiated power from the scattering coefficient alone. These statements could be represented mathematically as: $P_{in} - P_{reflected} = P_{radiated} + P_{ohmic}$. In an antenna, the reflected power is to be minimized while the radiative absorption is to be maximized, but again, ohmic absorption is to be minimized.

C.2 Antenna Measurements

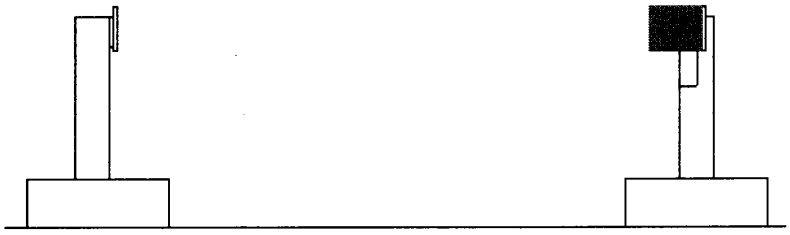

Figure C.2.1 Antenna Anechoic Test Chamber. The antenna on the left is the receiver calibrated antenna, the one on the right is the antenna under test.

Figure C.2.1 shows a typical setup for measuring the radiation pattern of an antenna. The setup incorporates a receiving and a transmitting antenna in an anechoic chamber. The anechoic chamber's walls covered with absorbers to absorb microwave radiation, thus preventing multi-path reflections, which would disturb the measurements. In this setup, the receiving antenna is stationary, with the main lobe pointing towards the transmitting antenna. The receiving antenna is calibrated in a sense that the radiation pattern and gain are assumed to be known. The transmitting antenna is the antenna under test; it is placed on a rotating stage which is controlled by a computer through a GPIB environment. A single frequency signal with a known power is generated via a frequency synthesizer.

The synthesizer is connected to the transmitting antenna through a matched coaxial cable. The receiving antenna is connected through a matched coaxial cable to a power meter. The power meter and synthesizer are connected to the PC via a GPIB cable and a motor to move the antenna is connected to the PC as well. A program on the PC controls the antenna position and takes distant measurements. The output is plotted and saved in a digital format for post-processing.

The antennas are far enough away so that the far field approximation can be observed. The radiation pattern is recorded as the receiving antenna is rotated at a particular path. This path gives a cross-section pattern such as the one in Figure C.1.1. Multiple patterns can be taken in order to render a more complete radiation characterization, i.e. the horizontal or vertical planes.

For polarization measurements, the receiving antenna is chosen to have a linear polarization and the antenna is rotated around its axis. This is accomplished by using a rotary joint and additional motor that rotates the antenna at a fixed speed. If sufficient number of data points is taken during one revolution, the difference between maximum and minimum readings will correspond to the axial ratio, i.e. if it is a circular polarized antenna, this should be 3dB.

REFERENCES

[1] M. Riaziat, S. Bandy, G. Zdasiuk, "Coplanar Waveguides for MMICs", Microwave Journal, pp. 125-131, June 1977

[2] Rainee N. Simons, Richard Q. Lee, Kurt A. Shalkhauser, Jonathan Owens, James Demarco, Joan Leen, Dana Sturzebecher, "Finite Width Coplanar Waveguide Patch Antenna With Vertical Fed Through Interconnect", NASA Tech Brief, LEW-16666, Linthicum Heights, MD.

[3] Ching-Cheng Tien, Ching-Kuang C. Tzuang, S. T. Peng, Chung-Chi Chang, "Transmission Characteristrics of Finte-Width Conductor-Backed Coplanar Waveguide", IEEE Transactions on Microwave Theory and Techniques, Vol. 41, No.9, pp. 1616-1624, Septermber 1993.

[4] Matthew Fillick, Ian D. Robertson, Jai S. Joshi, "An Analytical Method for Direct Calculation of E & H-Field Patterns of Conductor-Backed Coplanar Waveguide", IEEE Transactions on Microwave Theory and Techniques, Vol. 41, No. 9, pp. 1606-1610, September 1993.

[5] Jiri Svacina, "A Simple Quasi-Static Determination of Basic Parameters of Multilayer Microstrip and Coplanar Waveguide", IEEE Transactions on Microwave Theory and Techniques, Vol. 2, No. 10, pp. 385-387, October 1992.

[6] M. Riaziat, I. J. Feng, R. Majidi-Ahy, B. A. Auld, "Single-Mode Operation of Coplanar Waveguides", Electronics Letters, Vol 23, No. 24, pp. 1281-1283, November 1987.

[7] Majid Riaziat, Reza Majidi-Ahy, I-Jaung Feng, "Propagation Modes and Dispersion Characteristics of Copanar Waveguides", IEEE Transactions on Microwave Theory and Techniques, Vol. 38, No. 3, pp. 245-251, March 1990.

[8] T. Q. Deng, M. S. Leong, P. S. Kooi, T. S. Yeo, "Synthesis Formulas Simplify Coplanar-Waveguide Design", Microwaves & RF, pp. 84-97, March 1997.

[9] Said S. Bedair, Ingo Wolff, "Fast, Accurate and Simple Approximate Analytic Formulas for Calculating the Parameters of Supported Coplanar Waveguides for (M)MIC's", IEEE Transactions on Microwave Theory and Techniques, Vol. 40, No. 1, pp. 41-48, January 1992.

[10] Kwok K. M. Cheng, Jeremy K. A. Everard, "A New Technique for the Quasi-TEM Analysis of Conductor-Backed Coplanar Waveguide Structures", IEEE Transactions on Microwave Theory and Techniques, Vol. 41, No. 9, pp. 1589-1592, September 1993.

[11] Y. C. Shih, T. Itoh, "Anallysis of Conductor-Backed Coplanar Waveguide", Electronics Letters, Vol. 18, No. 12, pp. 538-539, June 1982.

[12] Shao-Jun Fang, Bai-Suo Wang, "Analysis of Asymmetric Coplanar Waveguide with Conductor Backing", IEEE Transactions on Microwave Theory and Techniques, Vol. 47, No. 2, pp. 238-240, February 1999.

[13] G. Ghione, C. Naldi, "Parameters of Coplanar Waveguides with Lower Ground Plane", Electronic Letters, Vol. 19, No. 18, pp. 734-735, September 1983.

[14] C. Veyres, V. Fouad Hanna, "Extension of The Application of Conformal Mapping Techniques to Coplanar Linews With Finite Dimentions", Int. J. Electronics, Vol. 48, No. 1, pp. 47-56,

[15] C. H. Wu, S. Uysal, "A New Systematic and Efficient Method of Analysis for Conductor-Backed Coplanar-Waveguide Directional Couplers", IEEE Transactions on Microwave Theory and Techniques, Vol. 47, No. 7, July 1999.

[16] Ramesh Garg, "Design Equations for Coupled Microstrip Lines", Int. J. Electronics, Vol. 47, No. 6, pp. 587-591, 1979.

[17] Manfred Kirschning, Rolf H. Jansen, "Accurate Wide-Range Design Equations for the Frequency-Dependent Characteristic of Parallel Coupled Microstrip Lines", IEEE Transactions on Microwave Theory and Techniques, Vol. MTT-32, No. 1, pp. 83-90 January 1984.

[18] J. H. Hinton, "On Design of Coupled Microstrip Lines", IEEE Transactions on Microwave Theory and Techniques, Vol. MTT-28, No. 3, pp. 272, March 1980.

[19] Sina Akhtarzad, Yhomas R. Rowbotham, Peter B. Johns, "The Design of Coupled Microstrip Lines", IEEE Transactions on Microwave Theory and Techniques, Vol. MTT-23, No. 6, pp. 486-492, June 1975.

[20] Wolfgang Hilberg, "From Approximations to Exact Relations for Characteristic Impedances", IEEE Transactions on Microwave Theory and Techniques, Vol. MTT-1, No. 5, pp. 259-265, May 1969.

[21] Jeffrey B. Knorr, Klaus-Dieter Kuchler, "Analysis of Coupled Slots and Coplanar Strips on Dielectric Substrate", IEEE Transactions on Microwave Theory and Techniques, Vol. MTT-23, No. 7, pp. 541-548, July 1975.

[22] Kenneth D. Marx, "Propagation Modes, Equivalent Circuits, and Characteristic Terminations for Multiconductor Transmission Lines with Inhomogeneous Delectrics", IEEE Transactions on Microwave Theory and Techniques, Vol. MTT-21, No. 7, pp450-457, July 1973.

[23] A. I. Grayzel, "A Useful Identity for the Analysis of Coupled Transmission-Line Structures", IEEE Transactions on Microwave Theory and Techniques, pp. 904-907, October 1974.

[24] A. I. Grayzel, "The Admittance Matrix of Coupled Transmission Lines", IEEE Transactions on Microwave Theory and Techniques, pp. 902-904, October 1974.

[25] A. Van de Capelle, "Transmission-line model for rectangular micrstrip antenna", *Handbook of Microstrip Antennas Vol 1*, edited by J. R. James, P. H. Hall, Chapter 10, London, United Kingdom, Peter Peregrinus Ltd., 1984.

[26] R. Collin, F. Zucker, *Antenna Theory*, New York, New York, McGraw-Hill, 1969.

[27] J. Helszajn, *Microwave Planar Passive Circuits and Filters*, West Essex, England, John Willey & Sons, 1994.

[28] Balanis, Contantine A., *Antenna Theory Analysis & Design*, New York, New York, John Wiley & Sons Inc., 1997.

[29] Roger F. Harrington, *Field Computation by Moment Methods*, New York, New York, The Macmillan Company, 1968.

[30] Warren L. Stutzman, Gary A. Thiele, *Antenna Theory and Design*, New York, New York, John Wiley & Sons, Inc. 1998.

[31] Max Ammann, "Design of Rectangular Microstrip Patch Antennas for the 2.4 GHz Band", Applied Microwave & RF, Vol. 9, No. 6, pp. 24-34, 1997.

[32] Shih-Chang Wu, Hung-Yu Yang, Nicolaos G. Alexopoulos, Ingo Wolff, "A Rigorous Dispersive Characterization of Microstrip Cross and T Junctions", IEEE Transactions on Microwave Theory and Techniques, Vol. 38, No. 12, pp. 1837-1844, December 1990.

[33] Boris Kapilevich, Roman Lukyanets, "Modeling Varactor Tunable Microstrip Resonators for Wireless Applications", Applied Microwave & Wireless, Vol. 10, No. 7, pp. 32-44, September 1998.